The Pattern of Coronary Arteriolar Bifurcations and the Uniform Shear Hypothesis

GHASSAN S. KASSAB and YUAN-CHENG B. FUNG

Institute for Biomedical Engineering, University of California, San Diego, La Jolla, CA

Abstract—By minimizing the cost function, which is the sum of the friction power loss and the metabolic energy proportional to blood volume, Murray derived an optimal condition for a vascular bifurcation. Murray's law states that the cube of the radius of a parent vessel equals the sum of the cubes of the radii of the daughters. We tested Murray's law against our data of pig's maximally vasodilated coronary arteriolar blood vessels at bifurcation points in control and hypertensive ventricles. Data were obtained from 7 farm pigs, 4 normal controls and 3 with right ventricular hypertrophy induced by stenosis of a pulmonary artery. Data on coronary arteriolar bifurcations were obtained from histological specimens by optical sectioning. The experimental results show excellent agreement with Murray's law in control and hypertensive hearts. Theoretically, we show that Murray's law can be derived alternatively as a consequence of the uniform vessel-wall shear strain rate hypothesis and a fluid mechanics equation based on conservation of mass and momentum. Conversely, the fluid mechanical equation, together with Murray's law, established as an empirical equation of actual measurements implies the uniformity of the shear strain rate of the blood at the vessel wall throughout the arterioles. The validity of these statements is discussed.

Keywords—Heart, Coronary arterioles, Murray's law, Shear strain rate, Shear stress, Right ventricular hypertrophy.

INTRODUCTION

The pattern of vascular trees has been studied by anatomists for years. In recent years physiologists have borrowed the methods of geographers and hydrologists to describe the bifurcation pattern of vascular trees. In several new articles (11–13) we have introduced the connectivity matrix and a diameter-defined Strahler system to describe the coronary arteries and veins. From our data we can present a relationship between the diameters of blood vessels at every point of bifurcation. Such relationships have been proposed theoretically from the principle of minimum work by Murray (17) and Oka (19,20), the prin-

ciple of optimal design by Rosen (22), the principle of minimum blood volume by Kamiya and Togawa (7), and the principle of minimum total shear force on the vessel wall by Zamir (27,28). The role of shear stress was first pointed out by Thoma (24) and verified by Kamiya and Togawa (8) by *in vivo* experiments in dogs. Zamir (27,28) deduced that the shear is uniform throughout the arterial system according to his principle of minimum total shear force. The uniform shear concept has received strong support from detailed studies of coronary blood flow by Giddens *et al.* (3) and others. The recognition of the physiological and molecular biologic roles played by shear stress acting on the endothelial cells has provided a great impetus to recent vascular mechanics research, see references in Ref. 2.

Murray (17,18) was the first to arrive at a relationship between the diameter of mother and daughter vessels at every point of bifurcation. He proposed a cost function that is the sum of the rate at which work is done on the blood and the metabolic rate of the vessel. The former is the product of blood flow rate and pressure drop. The latter is assumed to be proportional to the volume of the blood. By minimizing the cost function, Murray derived an equation that states that the cube of the radius of a parent vessel equals the sum of the cubes of the radii of the daughters. This relation is known as Murray's law.

In this study we shall test the validity of Murray's law against our measured data on the diameters of maximally vasodilated coronary arterioles in the right and left ventricles of normal pigs and in the right ventricles of right ventricular hypertrophy pigs (11,13). We shall then discuss the interplay between Murray's law, Murray's cost function and minimum principle, and the uniform shear strain rate or shear stress hypotheses.

METHODS

Measurements

In Refs. 11 and 13, we have described in detail the methods of preparation and measurement of the coronary arterioles. Briefly, 7 farm pigs (Yorkshire and Durocs crosses) were used in this study. Four of these animals

were used as controls and 3 had right ventricular hypertrophy (RVH) induced by a stenosis of the pulmonary artery. A Silastic snare stenosed the pulmonary artery until the right ventricular systolic pressures were raised to 70–80 mm Hg. The snare was then fixed to maintain this degree of stenosis. The animals were allowed to recover for 5 weeks, during which time the right ventricular pressure was hypertensive and the muscle hypertrophied. The control and hypertrophic pigs of the same age (4-months-old) and weight (30.5 ± 1.3 kg) were then prepared for morphometric study. Briefly, the control and RVH hearts were KCl-arrested, adenosine-dilated, and perfused with freshly catalyzed silicone elastomer through their major coronary arteries. The arterial perfusion pressure was set initially at 130 mm Hg for 5 min and then lowered and maintained at 80 mm Hg until the elastomer was hardened, in approximately 70–80 min. The hearts were refrigerated in saline for several days to increase the strength of the polymer. A total of 12 plugs of myocardial tissue were removed from each of the left and right ventricles of 4 control pigs and a total of 12 plugs from the right ventricles of 3 RVH pigs. Each plug was approximately 4 × 4 mm in cross-section and extended from epicardium to endocardium. Each plug was mounted on a freezing microtome and serially sectioned, transverse to the radial direction, to thicknesses of 60 to 80 μm from epicardium to endocardium. Each section was dehydrated with 100% alcohol and cleared with methyl salicylate to render the myocardium transparent and the silicone elastomer-filled microvasculature visible in light microscopy. The arterioles, venules, and capillaries were distinguished on the basis of their topography (10–12). The topography of the arterioles is tree-like, that of venules is root-like, whereas the capillaries have cross-connections. Morphometry of the arterioles was performed by changing the focal plane through the thickness of the histological section (optical sectioning). An image-processing system described in Ref. 11 was used to measure the dimensions. The arterioles were viewed, along their longitudinal direction, with an inverted light microscope (Olympus, optical resolution 0.6 μm at ×600 magnification) and displayed on a color video monitor (Sony Trinitron) through a television camera (COHU solid-state camera). The image was grabbed by the computer software and analyzed with a digitizing system. Several lumen diameter measurements were made along each vessel segment to obtain a mean diameter as shown in Fig. 1. Figure 2 shows an example of a reconstructed arteriolar tree from the left ventricle.

Analysis

Mathematically, consider a node connecting three vessels. We shall use the terms parent vessel and daughter vessels to denote the largest and the two smaller vessels
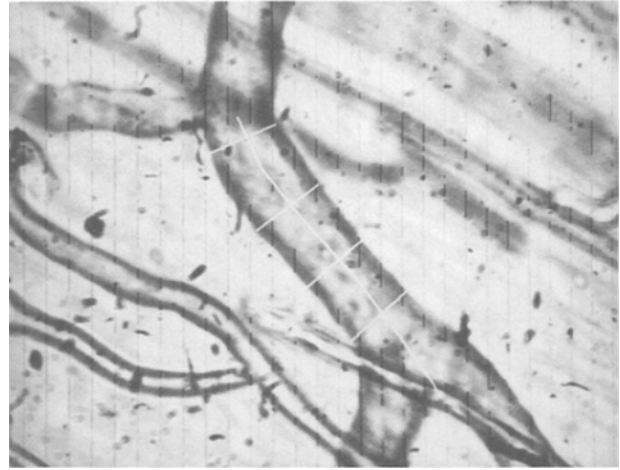

FIGURE 1. A reconstruction of a left ventricle arteriole showing the diameters measured along each vessel segment.

meeting at a node. We assume that blood is an incompressible Newtonian viscous fluid so that the flow is governed by the Navier–Stokes equation. The boundary condition is no-slip on the vessel wall. We assume that each vessel is a straight circular cylindrical tube and that the flow is laminar (*i.e.*, not turbulent), uniaxial (*i.e.*, the velocity is such that only the axial component is not identically zero), and unchanging in the axial direction. The last hypothesis is valid in an infinitely long tube but is rigorously nonvalid at the junction of three vessels. However, this hypothesis was used by Kamiya and Togawa (7), Murray (17,18), Oka (19,20), Rosen (22), and Zamir (27,28). Under these hypotheses the wall shear stress is proportional to flow over radius cube,

$$Q = (\pi a^3/4\mu)\, \tau_w, \qquad (1)$$

where Q is the rate of volume flow, a is the radius of the vessel, μ is the coefficient of viscosity of blood, and τ_w is the shear stress evaluated at the vessel wall. This relationship between blood flow and wall shear stress is valid for
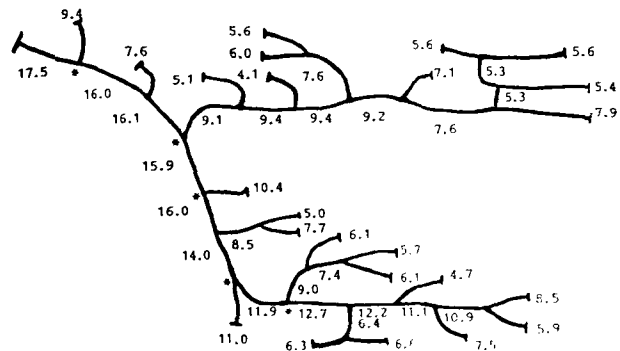
FIGURE 2. A schematic diagram of an arteriolar bifurcation to indicate the notation used.

each vessel. The principle of conservation of mass applied to the three vessels of a bifurcation gives, for an incompressible fluid,

$$Q_0 = Q_1 \pm Q_2, \qquad (2)$$

where the subscript 0 refers to the mother vessel and 1 and 2 refer to the daughter vessels. Using Eqs. 1 and 2, we obtain the desired relation

$$(a_0^3/\mu_0) \, \tau_{w0} = (a_1^3/\mu_1) \, \tau_{w1} + (a_2^3/\mu_2) \, \tau_{w2} \qquad (3)$$

or

$$a_0^3 \gamma_0 = a_1^3 \gamma_1 + a_2^3 \gamma_2 \qquad (4)$$

where γ_0, γ_1, γ_2, τ_{w0}, τ_{w1}, τ_{w2}, and μ_0, μ_1, μ_2 refer to the values of γ, τ_w, and μ at the boundaries of the tubes 0, 1, 2, respectively. Now, if one introduces the hypothesis that the shear strain rate or the coefficients of viscosity and the wall shear stresses are the same in all three vessels, then Eqs. 3 and 4 become

$$a_0^3 = a_1^3 + a_2^3 \qquad (5a)$$

or in terms of diameters,

$$D_0^3 = D_1^3 + D_2^3 \qquad (5b)$$

This is Murray's Law which can be rewritten as

$$D_1/D_0 = \{1/[1 + (D_2/D_1)^3]\}^{1/3} \qquad (6)$$

or

$$D_2/D_0 = \{(D_2/D_1)^3/[1 + (D_2/D_1)^3]\}^{1/3} \qquad (7)$$

Without loss of generality, we may set $D_1 \geq D_2$ by definition. We shall test our experimental data against Eqs. 6 and 7.

On the other hand, Murray (17) derived his Eq. 5 by minimizing a cost function of flow in a tube of length L:

Murray's cost function $= (8\mu L/\pi a^4)Q^2 + K_b\pi a^2 L, \qquad (8)$

in which the first term represents the work done by a Poiseuille flow, and the second term represents the metabolic cost proportional to the volume of the blood in the vessel in which K_b is a constant. According to Murray's minimum principle, for a given vessel of length L and flow Q there is an optimal radius a, which can be calculated by optimizing Eq. 8

$$Q = (\pi^2 K/16 \, \mu)^{1/2} \, a^3. \qquad (9)$$

On substituting Eq. 9 into the law of conservation of mass, Eq. 2, we obtain Murray's law (see Ref. 1, p. 87).

RESULTS

We have measured the diameters of all coronary arteries and arterioles of several right and left ventricles of four normal pigs and three right ventricular hypertrophic pigs.

The present right ventricular hypertrophy (RVH) was induced by stenosis of the pulmonary artery for 5 weeks (13). The mean and peak systolic pressures of the right ventricle increased to three to four times the control levels, and the right ventricle/left ventricle weight ratio doubled over the 5 weeks (13).

A total of 112 and 144 arteriole trees were measured from the left and right ventricles, respectively, of 4 normal pigs and a total of 160 arteriole trees from the right ventricles of 3 RVH pigs. Only those vessels with diameters in the range from 9 to 50 μm are considered in the present analysis. An example of an arteriolar tree with nodes having branches lying is this range is shown in Fig. 2 with the nodes identified by asterisks. We obtained data from a total of 489 and 1,193 arteriolar nodes from the left and right ventricles, respectively, of normal pigs and a total of 1,007 arteriolar nodes from the right ventricles of RVH pigs.

Figures 3A and 3C show the branch diameter ratios D_1/D_0 and D_2/D_0 plotted against the daughter vessels diameter ratio D_2/D_1 for the left ventricles. The data points correspond to the experimental measurements, whereas the solid curves correspond to the theoretical formulas, Eqs. 6 and 7. Figures 3B and 3D show the same data averaged over D_2/D_1 intervals of 0.05. Similarly, Figs. 4A–4D show the data for the control right ventricles, while Figs. 5A–5D show the corresponding data for the hypertensive right ventricles. The theoretical predictions agree with the experimental data within the ±95% confidence limits.

We may further determine the agreement between the theoretical predictions and experimental measurements by examining the deviation of $[D_1^3 + D_2^3]/D_0^3$, Eq. 5, from unity as proposed by Lipowsky (15). Figures 6a–6c show the distributions for the various bifurcations of the left and right ventricles of normal pigs and right ventricles of RVH pigs, respectively. The mean ± SE for the left and right ventricles of normal pigs are 1.03 ± 0.015 and 1.05 ± 0.0096, respectively, and 1.10 ± 0.0097 for the right ventricles of RVH pigs.

We conclude that Eqs. 5, 6, and 7, or Murray's law, is valid in the statistical sense for the maximally vasodilated coronary arterioles in normal right and left ventricles of the pig and in the hypertrophic right ventricles of the pigs examined. Murray's law, Eq. 5, is then a good empirical formula of the experimental data.
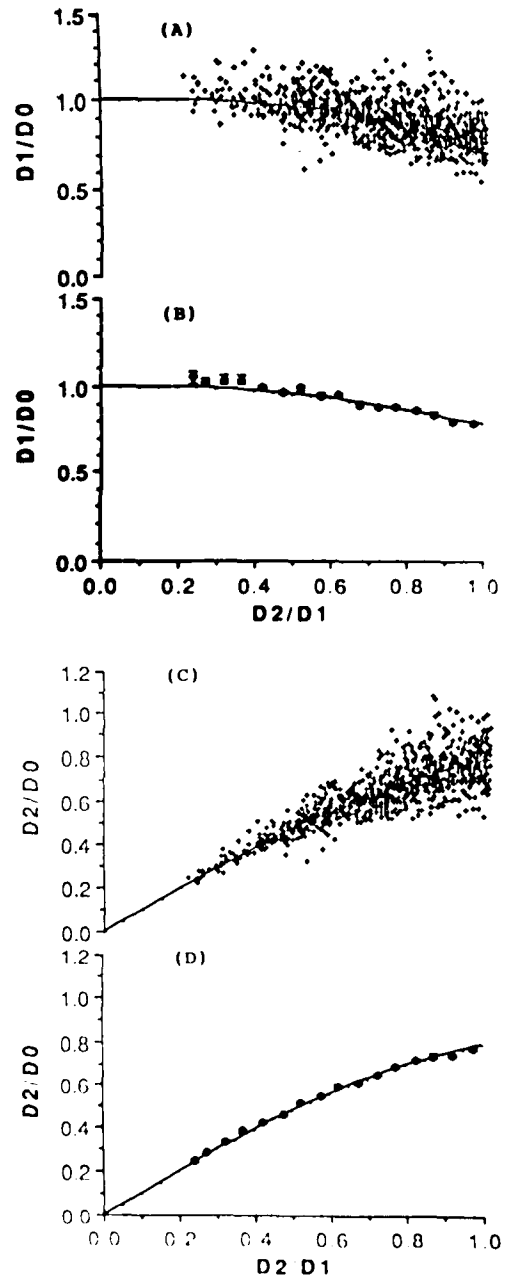
DISCUSSION

Comparison with Other Works

Murray's law of cubic dependence of blood flow on vessel diameter has been validated by Mayrovitz and Roy (16) in the cremaster muscle microvasculature of normotensive and hypertensive rats. Murray's law of diame-
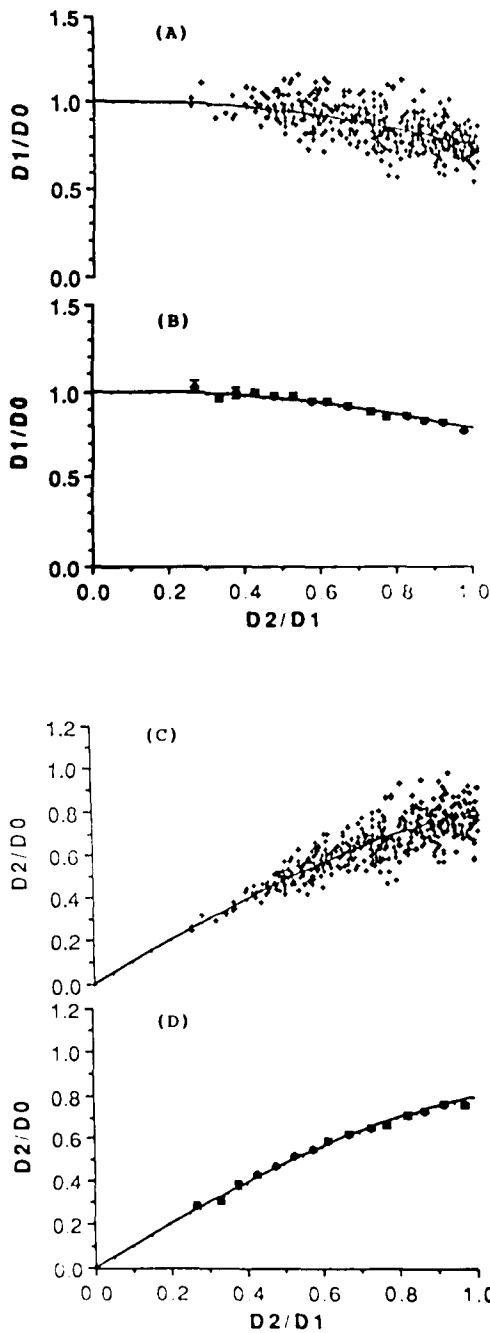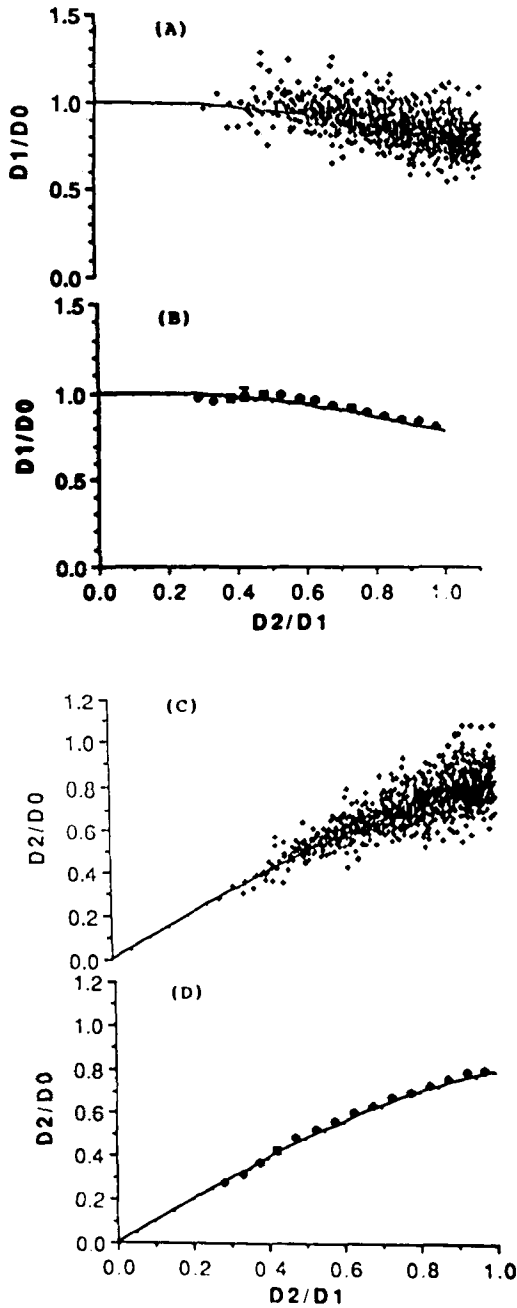
FIGURE 3. (A) Measured data of arteriolar bifurcations of left ventricles of normal pigs compared with Eq. 8. A diameter ratio of the larger branch to parent vessel (D_1/D_0) plotted against the diameter ratio of daughter branches, (D_2/D_1). (B) Mean ± SE of same data averaged over D_2/D_1 intervals of 0.05. (C) Diameter ratio of the smaller branch to parent vessel (D_2/D_0) plotted against (D_2/D_1). (D) Mean ± SE of same data averaged over D_2/D_1 intervals of 0.05.

FIGURE 4. (A) Measured data of arteriolar bifurcations of right ventricles of normal pigs compared with Eq. 8. A diameter ratio of the larger branch to parent vessel (D_1/D_0) plotted against the diameter ratio of daughter branches, (D_2/D_1). (B) Mean ± SE of same data averaged over D_2/D_1 intervals of 0.05. (C) Diameter ratio of the smaller branch to parent vessel (D_2/D_0) plotted against (D_2/D_1). (D) Mean ± SE of same data averaged over D_2/D_1 intervals of 0.05.

ters has also been tested for arterial bifurcations in the retina of man and monkey (29,30), in various parts of the cardiovascular system of man, rabbit, and pig (31), and in the coronary arteries of man and rat (32,33). The caliber

of vessels examined in these studies were >50 μm in diameter. Rough validity was shown but the scatter was large. It should be noted, however, that Poiseuille's formula was postulated in the derivation of Murray's law. In theory, Poiseuille's formula applies only to steady laminar flow, without turbulence and at zero Womersley's num-

FIGURE 5. (A) Measured data of arteriolar bifurcations of right ventricles of RVH pigs compared with Eq. 8. A diameter ratio of the larger branch to parent vessel (D_1/D_0) plotted against the diameter ratio of daughter branches, (D_2/D_1). (B) Mean ± SE of same data averaged over D_2/D_1 intervals of 0.05. (C) Diameter ratio of the smaller branch to parent vessel (D_2/D_0) plotted against (D_2/D_1). (D) Mean ± SE of same data averaged over D_2/D_1 intervals of 0.05.

bers. These conditions are best approximated in smaller vessels. Hence, in our study we have considered only those arterial vessels <50 μm in diameter, see Figs. 3–5. It is not surprising that the scatter of data is smaller in our study, for vessels <50 μm in diameter, than that of pre-

vious studies, for vessels >50 μm in diameter (32,33). House and Lipowsky (5) also examined vessels <50 μm and reported good agreement with Murray's law for the rat cremaster muscle microcirculation. However, no data were presented since the focus of their study was on the microvascular hematocrit and red cell flux.

Murray's Minimum Cost Function and the Uniform Wall Shear Hypothesis

Murray derived his morphological statement (Murray's law) from a theory of minimum cost. We showed that Murray's law can be derived alternatively as a consequence of the uniform vessel wall shear strain rate hypothesis and a fluid mechanics equation based on conservation of mass and momentum. Murray's law, however, implies the uniformity of shear stress since on comparing Eq. 1 with Eq. 9, we obtain

$$\tau_w = (K_b\mu)^{1/2} \tag{10}$$

If K_b and μ are the same in all vessels, then τ_w is uniform in all vessels. Hence we see when using Poiseuille's formula in Murray's cost function the minimum principle leads to Eqs. 5 and 10, *i.e.*, Murray's law and the uniformity of shear stress.

If we don't use the minimum principle but use Poiseuille's law and the hypothesis of uniform shear stress, then by introducing the latter into Eq. 3, we obtain Murray's law, Eq. 5. Thus Murray's law follows Poiseuille's formula, the law of conservation of mass, and the uniform shear hypothesis. Conversely, if Murray's law, Eq. 5, is accepted as an empirical equation from morphometry, and Poiseuille's formula and conservation of mass are accepted, then Eq. 4 is valid. The simultaneous validity of Eqs. 4 and 5 implies, on eliminating a_0^3, that

$$(\gamma_1 - \gamma_0) a_1^3 = (\gamma_2 - \gamma_0) a_2^3. \tag{11}$$

This equation can be valid for arbitrary values of a_1 and a_2 only if

$$\gamma_0 = \gamma_1 = \gamma_2. \tag{12}$$

That is, the strain rate at the wall is uniform in all three vessels. Another way to look at this is to think of γ as a parameter for each vessel. According to Poiseuille's formula $\pi\gamma_0/4$, $\pi\gamma_1/4$, and $\pi\gamma_2/4$ are equal to Q_0/a_0^3, Q_1/a_1^3, and Q_2/a_2^3, respectively. Using them in Eq. 4 yields Eq. 2. Using them in Eq. 5 yields

$$Q_0/\gamma_0 = Q_1/\gamma_1 + Q_2/\gamma_2. \tag{13}$$

Equations 13 and 2 can be valid simultaneously for arbitrary Q_2/Q_1 only if Eq. 12 holds.

The uniform shear hypothesis has an interesting implication for the viscous energy dissipation. The volumetric
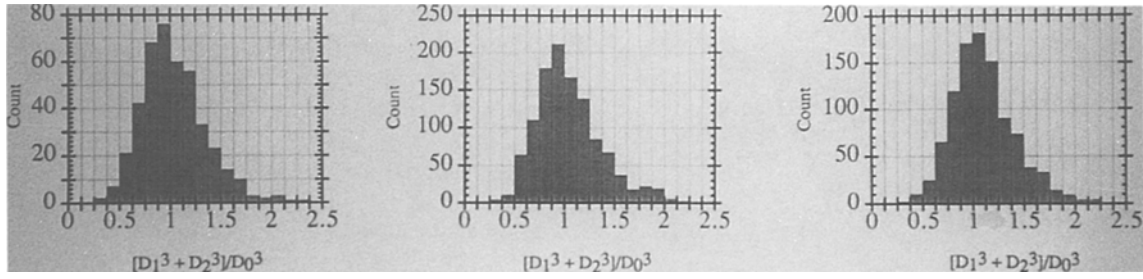
FIGURE 6. (A) Histogram of the ratio of sum of the cubes of daughter branch diameters to that of the parent branch for the arteriolar bifurcations of left ventricles of normal pigs. (B) Histogram of the ratio of sum of the cubes of daughter branch diameters to that of the parent branch for the arteriolar bifurcations of right ventricles of normal pigs. (C) Histogram of the ratio of the sum of the cubes of daughter branch diameters to that of the parent branch for the arteriolar bifurcations of right ventricles of RVH pigs.

rate of viscous dissipation at the vessel wall, Φ, is the product of wall shear stress and strain rate,

$$\Phi = \tau_w \gamma_w. \tag{14}$$

However, since the shear stress is the product of fluid viscosity and strain rate, Eq. 14 becomes

$$\Phi = \mu\gamma_w^2. \tag{15}$$

Hence, the viscous energy dissipation along the vessel wall is equal to the product of viscosity and the square of the wall shear strain rate. This implies uniform energy dissipation throughout the arteriolar walls if the fluid viscosity and wall shear stress are constant.

The hypothesis of uniform blood shear stress acting on the blood vessel wall has been supported by several studies. Kamiya and Togawa (8) surgically constructed an arteriovenous shunt from the common carotid artery to the external jugular vein, caused an increase of blood flow in one segment of the artery and a decrease of flow in another. They then showed that in 6 to 8 months after the operation, the segment with increased flow dilated while the other segment with decreased flow atrophied to a smaller diameter. The diameter of the artery was increased or decreased in such a way that the wall shear rate remained almost constant if the change of flow was within four times of the control. Constant shear rate implies constant shear stress if the viscocity is constant. Thoma (24), Liebow (14) and others, on observing embryologic vascular development and studying arteriovenous fistulas and collateral circulation, have shown that increased blood flow induces blood vessel dilatation. Rodbard (21) collected clinical evidence of the same. More recently, Kamiya et al. (9) and Giddens et al. (3) have collected data from literature and their own research and concluded that the blood arterial shear stress acting on the walls of dog's peripheral and coronary arterioles, arteries, and aorta lies in the range of 10–20 dynes/cm^2. The narrowness of the range of wall shear stress is remarkable.

The shear strain rate and shear stress on blood vessel wall discussed in Refs. 7, 17–20, 22, 24, and 28 are those

evaluated by Poiseuille's formula pertaining to a cylindrical tube with a smooth inner wall. The actual inner wall of a blood vessel is the endothelium, which is not smooth. Taking the bumpiness of the endothelium into account, Yamaguchi et al. (26) have shown that the actual shear stress on the endothelial cell wall is nonuniform even though the flow is uniform. The reason is that the flow has no slip on the endothelial cell wall, on which the relative velocity is zero; consequently the displacement of the surface of the wall constitutes a nontrivial pertubation of flow in the neighborhood of the wall. Further, the blood shear stress is an external load acting on the endothelial cells. A uniform external load does not imply a uniformity of the stress and strain in the endothelial cells. In fact, the tensile stress and shear stress in the endothelial cell membrane can be very large and nonuniform even when the external loading is small and uniform, as is discussed in Fung and Liu (2).

Other Cost Functions

Oka (19) generalized Murray's cost function by adding another term of metabolic cost proportional to the volume of the blood vessel wall. Hence, Murray's modified cost function, P, has the form

$$P = (8\mu L/\pi a^4)\, Q^2 + K_b\, \pi a^2 L + K_w\, 2\pi a h L \tag{16}$$

where K_w and h are the metabolic constant and thickness of the vessel wall, respectively, and are assumed to be constant. Optimization of Eq. 16 with respect to radius a yields

$$Q = (\pi^2 K_b/16\, \mu)^{1/2}\, a^3[1 + \alpha/a]^{1/2},$$
$$\alpha = hK_w/K_b. \tag{17}$$

On substituting Eq. 17 into the law of conservation of mass, Eq. 2, we obtain Oka's (19) modified Murray's law

$$a_0^3[1 + \alpha/a_0]^{1/2} = a_1^3[1 + \alpha/a_1]^{1/2} + a_2^3\, [1 + \alpha/a_2]^{1/2}. \tag{18}$$

The constant α was determined from our morphometric data for various bifurcations. The values of α were found

to be negative however, *i.e.*, nonphysical. This can be seen analytically when considering some special cases. In the asymmetric case where $a_0 = a_1 > a_2$, the solution to Eq. 18 becomes $\alpha = -a_2$. Also, in the symmetric case where $a_1 = a_2$, the solution to Eq. 18 becomes $[a_0{}^6 - 4a_1{}^6]/[4a_1{}^5 - a_0{}^5]$. It can easily be shown that this expression also takes on negative values since $a_0 \geq a_1$.

Next, consider a cost function that is the sum of the friction power loss and the metabolic energy proportional to vessel wall volume only (*i.e.*, Eq. 16 without the second term). Furthermore, we remove the hypothesis that the vessel thickness is a constant, independent of diameter. Tomanek *et al.* (25) have measured wall thicknesses for various caliber coronary arterial vessels in the dog. Their data can be fitted with a least square fit: $h = 1.06a^{0.457}$ ($R^2 = 9.65$) for our diameter range of interest. It can be shown that substitution of this expression into our cost function, followed by optimization, will yield the result that the flow is proportional to $a^{2.73}$. This result differs from Murray's law in that the exponent of radius is 2.73 instead of 3. Conservation of mass along a bifurcation yields a result similar to Murray's law: $D_0{}^{2.73} = D_1{}^{2.73} + D_2{}^{2.73}$. This relation was also tested against our morphological data and was found to be in good agreement. We also found the mean ± SE of the function $[D_1{}^{2.73} + D_2{}^{2.73}]/D_0{}^{2.73}$ to be 1.08 ± 0.015 and 1.09 ± 0.0091 for the left and right ventricles of normal pigs, respectively, and 1.14 ± 0.0089 for the right ventricles of RVH pigs. Suwa *et al.* (23) found the average exponent to have a similar value of 2.7 from data obtained from acrylic resin arterial casts of a variety of human organs. Hutchins *et al.* (6) found a mean value for the exponent of 3.2 for the left main coronary artery and its branches (diameter range of 1.0–3.3 mm) obtained from postmortem human coronary arteriograms while cast measurements of sheep bronchi diameters yielded a value of 2.98 for the exponent (4). Finally, Mayrovitz and Roy (16) found the exponent to have a mean value of 3.01 for the rat cremaster muscle microvasculature.

The minimum cost of principle is a hypothesis (an axiom). Each expression of cost function is an additional hypothesis. Any extra mathematical or empirical simplification of the cost function is a further additional hypothesis. Hence, validation is needed when proposing and optimizing cost functions.

REFERENCES

1. Fung, Y. C. *Biodynamics: Circulation*. Springer Verlag: New York, 1980.
2. Fung, Y. C., and S. Q. Liu. Elementary mechanics of the endothelium of blood vessels. *J. Biomech. Eng.* 115:1–12, 1993.
3. Giddens, D. P., C. K. Zarins, and S. Glagov. Response of arteries to near-wall fluid dynamic behavior. *Appl. Mech. Rev.* 43:S98–S102, 1990.
4. Hooper, G. Diameters of bronchi at asymmetrical divisions. *Respir. Physiol.* 31:291–294, 1977.
5. House, S. D., and H. H. Lipowsky. Microvascular hematocrit and red cell flux in rat cremaster muscle. *Am. J. Physiol.* 252(Heart Circ. Physiol. 21):H211–H222, 1987.
6. Hutchins, G. M., M. M. Miner, and J. K. Boitnott. Vessel caliber and branch angle of human coronary artery branch points. *Circ. Res.* 38:572–576, 1976.
7. Kamiya, A., and T. Togawa. Optimal branching structure of the vascular tree. *Bull. Math. Biophys.* 34:431–438, 1972.
8. Kamiya, A., and T. Togawa. Adaptive regulation of wall shear stress to flow change in the canine carotid artery. *Am. J. Physiol.* 239(Heart Circ. Physiol.) 8:H14–H21, 1980.
9. Kamiya, A., R. Bukhari, and T. Togawa. Adaptive regulation of wall shear stress optimizing vascular tree function. *Bull. Math. Biol.* 46:127–137, 1984.
10. Kassab, G. S., and Y.-C. Fung. Topology and dimensions of pig coronary capillary network. *Am. J. Physiol.* 267(Heart Circ. Physiol. 36):H319–H325, 1994.
11. Kassab, G. S., C. A. Rider, N. J. Tang, and Y.-C. Fung. Morphometry of pig coronary arterial trees. *Am. J. Physiol.* 265(Heart Circ. Physiol. 34):H350–H365, 1993.
12. Kassab, G. S., Daniel H. Lin, and Y. C. Fung. Morphometry of pig coronary venous system. *Am. J. Physiol.* 267(Heart Circ. Physiol. 36):H2100–H2113, 1994.
13. Kassab, G. S., K. Imoto, F. C. White, C. A. Rider, Y.-C. Fung, and C. M. Bloor. Coronary arterial tree remodeling in right ventricular hypertrophy. *Am. J. Physiol.* 265(Heart Circ. Physiol. 34):H366–H375, 1993.
14. Liebow, A. A. Situations which lead to changes in vascular patterns. In: *Handbook of Physiology, Section 2:* Circulation, Vol. 2. Washington, D.C.: American Physiological Society, pp. 1251–1276, 1963.
15. Lipowsky, H. H. Rheological and topographical factors affecting shear stress in the microcirculation. *Adv. Bioeng. BED* 26:385–388, ASME, 1993.
16. Mayrovitz, H. N., and J. Roy. Microvascular blood flow: evidence indicating a cubic dependence on arteriolar diameter. *Am. J. Physiol.* 245(Heart Circ. Physiol. 14):H1031–H1038, 1983.
17. Murray, C. D. The physiological principle of minimum work. I. The vascular system and the cost of blood volume. *Proc. Nat. Acad. Sci. U.S.A.* 12:207–214, 1926.
18. Murray, C. D. The physiological principle of minimum work applied to the angle of branching of arteries. *J. Gen. Physiol.* 9:835–841, 1926.
19. Oka, S. *Biorheology*. Syokabo, Tokyo (in Japanese), 1974.
20. Oka, S. *Biorheology*. Syokabo, Tokyo (in Japanese), 1984.
21. Rodbard, S. Vascular caliber. *Cardiology* 60:4–49, 1975.
22. Rosen, R. *Optimality Principles in Biology*. London: Butterworth, 1967.
23. Suwa, N., N. Takashi, H. Fukasawa, and Y. Sasaki. Estimation of intravascular blood pressure gradient by mathematical analysis of arterial casts. *Tohoku J. Exp. Med.* 79: 168–198, 1973.
24. Thoma, R. *Untersuchungen uber die Histogenese und Histomechanik des Gefasssystemes*. Stuttgart: Enke, 1893.
25. Tomanek, R. J., P. J. Palmer, G. L. Peiffer, K. L. Schreiber, C. L. Eastham, and M. L. Marcus. Morphometry of canine coronary arteries, arterioles, and capillaries during

hypertension and left ventricular hypertrophy. *Circ. Res.* 58:38–46, 1986.

26. Yamaguchi, T., K. Hoshiai, H. Okino, A. Sakurai, S. Hanai, M. Masuda, and K. Fujiwara. On shear stress acting on the endothelium. Presented at 1993 Bioengineering Conference, Bioeng. Div. Vol. 24, ASME, p. 167.

27. Zamir, M. The role of shear forces in arterial branching. *J. Gen. Biol.* 67:213–222, 1976.

28. Zamir, M. Shear forces and blood vessel radii in the cardiovascular system. *J. Gen. Physiol.* 69:449–461, 1977.

29. Zamir, M., J. A. Medeiros, and T. K. Cunningham. Arterial bifurcations in the human retina. *J. Gen. Physiol.* 74: 537–548, 1979.

30. Zamir, M., and J. A. Medeiros. Arterial branching in Man and Monkey. *J. Gen. Physiol.* 79:353–360, 1982.

31. Zamir, M., and N. Brown. Arterial branching in various parts of the cardiovascular system. *Am. J. Anatomy* 163: 295–307, 1982.

32. Zamir, M., S. Phipps, B. L. Langille, and T. H. Wonnacott. Branching characteristics of coronary arteries in rats. *Can. J. Physiol. Pharmacol.* 62:1453–1459, 1984.

33. Zamir, M., and H. Chee. Branching characteristics of human coronary arteries. *Can. J. Physiol. Pharmacol.* 64: 661–668, 1986.